Available online at www.sciencedirect.com
ScienceDirect
Optik 119 (2008) 122–126
Optik Optics
www.elsevier.de/ijleo

Phase matching limitation of high-efficiency second-harmonic generation in both phase- and group-velocity-matched structures

Wei Han[a,*], Wan-Guo Zheng[a,b], Yi-Sheng Yang[a], Ding-Xiang Cao[a], Qi-Hua Zhu[a], Lie-Jia Qian[b]

[a]*Laser Fusion Research Center, CAEP, Mianyang, Sichuan 621900, China*
[b]*Department of Optical Science and Engineering, Fudan University, Shanghai 200433, China*

Received 14 April 2006; accepted 4 July 2006

Abstract

In this paper, we studied efficient second-harmonic generation (SHG) of femtosecond pulses in both phase- and group-velocity-matched structures. Obtained results show that phase matching becomes more critical under conditions required for high levels of conversion efficiency. And the imperfect phase mismatch caused by mismatched group-velocity dispersion (GVD) will limit conversion efficiency as well as bandwidth of generated second-harmonic (SH) pulses. The spectral characteristics of the generated SH pulses and its conversion efficiency in the strong pump regime are investigated in detail. The acceptance bandwidth of nonlinear crystal in the high-efficiency SHG is redefined in the paper, and the definition is much closer to the practical application of design.

Keywords: Frequency conversion; Femtosecond pulses; Group-velocity dispersion

1. Introduction

High-efficiency broadband frequency conversion through second-harmonic generation (SHG) is attracting increasingly research interest due to the advances of femtosecond lasers. For pulses of ~100 fs or shorter, group-velocity mismatch between fundamental-harmonic (FH) and its second-harmonic (SH) waves is a dominant factor limiting the performance of SHG, which leads to a temporal walk-off between FH and SH pulses, hence a lower conversion efficiency as well as a narrower bandwidth and/or longer duration of generated SH pulses [1,2]. Several approaches have been proposed and demonstrated to deal with the problems of group-velocity mismatch, such as achromatic phase matching [3–6], multi-crystal sequence [7], tilted quasi-phase-matched gratings [8], Cerenkov phase matching [9], etc. Unfortunately, these approaches are not possible to be used in practice due to the complexity and quite strict requirements for alignment of the optics. Thus it is interesting to propose new SHG structures with both phase matching (PM) and group-velocity matching (GVM), or search for special nonlinear crystals with zero group-velocity mismatch. Recently, a quasi-phase-matched and group-velocity-matched (QPM–GVM) scheme [10,11] has been proposed. In the QPM–GVM structure, crystals are cut at the GVM angle and the PM is satisfied through modulating the sign of nonlinear coefficients. In this case, the doubling configuration is just like the conventional one and no modifications of the input light are needed, which makes

*Corresponding author.
E-mail address: tongyhan2000@hotmail.com (W. Han).

0030-4026/$ - see front matter © 2006 Elsevier GmbH. All rights reserved.
doi:10.1016/j.ijleo.2006.07.006

it more practical in the sense of simplicity, reliability and conversion efficiency. On the other hand, several mature crystals were investigated and found to exit a vanished group-velocity mismatch wavelength of SHG, such as BBO for 1.5 μm [12], LBO for 1.3 μm [13], MgO-doped PPLN for 1.55 μm communication band [14], partially deuterated KDP for 1.034–1.179 μm region and potentially KDP analogs for 1.013–1.278 μm region [15]. Particularly, partially deuterated KDP will be of great concern since its zero group-velocity mismatch wavelength may be tuned with deuteration level and the large-size availability makes it more promising in high-power applications. For example, a deuteration level of 12% corresponds to the vanished group-velocity mismatch wavelength of 1.054 μm that matches with the emission wavelength of Nd:glass laser. Zhu et al. experimentally investigated SHG of high-intensity femtosecond pulses in a partially deuterated KDP around this wavelength. Conversion efficiency as high as 55% was achieved with a high-intensity ($\sim$5 GW/cm^2) Gaussian beam [16].

SHG in both PM and GVM structures is an important configuration for frequency conversion of femtosecond or broadband lasers. In this case, the conversion efficiency is limited by the imperfect phase matching resulting from both group-velocity dispersion (GVD) and from input fundamental pulse bandwidth. In order to achieve high conversion efficiency, the input FH bandwidth needs to be small compared with the acceptance bandwidth of the crystal. The acceptance bandwidth is determined by GVDs of FH and SH pulses in both PM and GVM SHG. Several papers have given the exact solution of the acceptance bandwidth under the assumption of no source depletion in the group-velocity mismatch SHG [10,17]. However, in both PM and GVM SHG, the conversion efficiency is usually high, and the former solution of acceptance bandwidth no longer holds true.

In this paper, we consider phase matching limitations on SHG due to GVD and input FH bandwidth. Calculations are done in the regime of the pump depletion. The obtained results show that PM becomes more critical under conditions required for high levels of conversion efficiency. And the imperfect phase mismatch caused by mismatched GVD will limit conversion efficiency as well as bandwidth of generated SH pulses. The acceptance bandwidth of nonlinear crystal in the high-efficiency SHG is redefined in the paper, and the definition is much closer to the practical application.

2. Theoretical model

Type-I SHG process can be treated by the nonlinear coupled-wave equations in time domain. To the first order in quadratic susceptibility $\chi^{(2)}$ and neglecting all derivatives of refraction index beyond the second, the equations that govern the envelopes E_1 and E_2 of FH and SH pulses, respectively, are

$$\frac{\partial E_1(z,t)}{\partial z}+\frac{1}{v_{g1}}\frac{\partial E_1(z,t)}{\partial t}-\frac{\mathrm{i}}{2}\beta_{21}\frac{\partial^2 E_1(z,t)}{\partial t^2}=-\frac{\mathrm{i}\omega_1 d_1}{n_1 c}E_2E_1^*\exp(-\mathrm{i}\,\Delta k z), \tag{1}$$

$$\frac{\partial E_2(z,t)}{\partial z}+\frac{1}{v_{g2}}\frac{\partial E_2(z,t)}{\partial t}-\frac{\mathrm{i}}{2}\beta_{22}\frac{\partial^2 E_2(z,t)}{\partial t^2}=-\frac{\mathrm{i}\omega_1 d_1}{n_2 c}E_1^2\exp(\mathrm{i}\,\Delta k z), \tag{2}$$

where v_{g1} (v_{g2}) and β_{21} (β_{22}) are group velocity and GVD parameters at FH (SH) frequency, respectively. $\Delta k(\omega_0)=2k_1-k_2$ is the phase mismatch at central frequencies.

It is convenient to transfer the above equations to a retarded frame of reference and further convert them into dimensionless forms by using parameters normalized to the corresponding input FH electric amplitude E_0, pulse duration t_0 and nonlinear length $L_{NL}=2n_1c/(\omega\chi^{(2)}E_0)$, respectively. The defined nonlinear length L_{NL} is a parameter measuring the input intensity. The resulted equations can be written as

$$\frac{\partial A_1}{\partial l}-\mathrm{sgn}(\beta_{21})\mathrm{i}\frac{L_{NL}}{2L_{D1}}\frac{\partial^2 A_1}{\partial\tau^2}=-\mathrm{i}A_2A_1^*\exp(-\mathrm{i}\,\Delta k L_{NL} l), \tag{3}$$

$$\frac{\partial A_2}{\partial l}+\frac{L_{NL}}{L_w}\frac{\partial A_2}{\partial\tau}-\mathrm{sgn}(\beta_{22})\mathrm{i}\frac{L_{NL}}{2L_{D2}}\frac{\partial^2 A_2}{\partial\tau^2}=-\mathrm{i}A_1^2\exp(\mathrm{i}\,\Delta k L_{NL} l), \tag{4}$$

where $A_i=E_i/E_0$, $l=z/L_{NL}$ and $\tau=(t-z/v_{g1})/t_0$. The GVM length, $L_w=t_0(1/v_{g2}-1/v_{g1})^{-1}$, is a length over which the FH and SH pulses separate by the pulse duration owing to GVM. We assume that the initial FH pulse is a Gaussian pulse $E(0,t)=E_0\exp(-t^2/t_0^2)$, thus the standard FWHM pulse width should read as $t_p=\sqrt{2\ln 2}t_0$. In this paper, we define the dispersion lengths as $L_{Di}=t_0^2/|\beta_{2i}|$ ($i=1,2$). The most concerned case in our numerical studies is the SHG of femtosecond pulses at 1.054 μm in a 12% deuterated KDP crystal with $\beta_{21}=-13\,\mathrm{fs}^2/\mathrm{mm}$ and $\beta_{22}=70\,\mathrm{fs}^2/\mathrm{mm}$, respectively. In this situation, PM and GVM between FH and SH pulses are satisfied simultaneously.

3. Numerical results and discussions

To study SHG of femtosecond pulses in both phase- and group-velocity matching structures, the coupled-wave equations are numerically solved by the standard

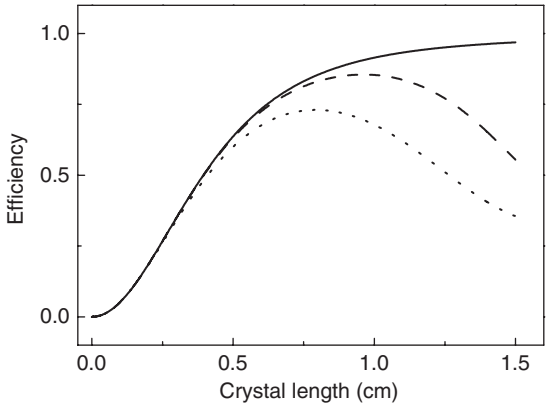

Fig. 1. Calculated conversion efficiency versus crystal length under high pump intensity ($L_{nl} = 3.5$ mm) for different values of FH bandwidth: (1) $\Delta\lambda_{FH} = 0$ (solid line), (2) $\Delta\lambda_{FH} = 31$ nm (dashed line) and (3) $\Delta\lambda_{FH} = 54$ nm (dotted line).

split-step approach. We first investigate the conversion efficiency dependence on the crystal length under high pump intensity for different values of FH bandwidth. The results are shown in Fig. 1. As expected, the conversion efficiency increases monotonically with the crystal length in the case of narrowband FH pulses. However, when the FH pulse is broadband, the conversion efficiency begins to decrease after increasing the crystal length beyond an optimal value. The drop of the conversion efficiency reveals a reconversion, namely energy retransferring back from SH pulses to FH pulses. Reconversion is due to the imperfect phase matching and pump depletion. In both phase- and group-velocity matching structures, the imperfect phase matching results from mismatched GVDs of FH and SH pulses (i.e., $\beta_{21}/\beta_{22} \neq 2$) and input bandwidth of FH pulse. This can be easily understood by investigating the phase matching condition on a broadband basis. The phase mismatch, $\Delta k(\omega)$, can be expanded around the central frequency of FH pulse:

$$\begin{aligned}\Delta k(\omega) &= k_2(2\omega) - 2k_1(\omega) = \Delta k(\omega_0) + 2\left(\frac{\partial k_2}{\partial\omega} - \frac{\partial k_1}{\partial\omega}\right)\Delta\omega \\ &+ \left(2\frac{\partial^2 k_2}{\partial\omega^2} - \frac{\partial^2 k_1}{\partial\omega^2}\right)\Delta\omega^2 + \frac{1}{3}\left(4\frac{\partial^3 k_2}{\partial\omega^3} - \frac{\partial^3 k_1}{\partial\omega^3}\right)\Delta\omega^3 \\ &+ \cdots = \Delta k(\omega_0) + 2\left(\frac{1}{v_2} - \frac{1}{v_1}\right)\Delta\omega \\ &+ (2\beta_{22} - \beta_{21})\,\Delta\omega^2 + \tfrac{1}{3}(4\beta_{32} - \beta_{31})\,\Delta\omega^3 + \cdots \\ &= (2\beta_{22} - \beta_{21})\,\Delta\omega^2 + \tfrac{1}{3}(4\beta_{32} - \beta_{31})\,\Delta\omega^3 + \cdots . \quad (5)\end{aligned}$$

When the PM and GVM are satisfied simultaneously, the higher-order phase mismatching is determined by GVD and third-order dispersion (TOD). In many common situations of SHG, the third-order phase mismatch is much smaller than the second-order term. For example, the TOD parameters at 1.054 μm in a 12% deuterated KDP crystal are calculated to be $\beta_{31} = 68\,\mathrm{fs}^3/\mathrm{mm}$ and $\beta_{32} = 30\,\mathrm{fs}^3/\mathrm{mm}$, respectively. Based on Eq. (5), it can be estimated that the contribution of TOD may be comparable to that of GVD only if sub-femtosecond pulses are involved. Thus, TOD can be neglected reasonably in our calculations. In this situation, the imperfect phase mismatch caused by GVD mismatch between FH and SH pulses dominates in the both PM and GVM SHG structures.

It is also clearly shown by Eq. (5) that if $\beta_{21}/\beta_{22} = 2$ is satisfied, the imperfect phase mismatch vanishes. In this case, reconversion will no longer exist, and conversion efficiency will increase monotonically with crystal length, as shown in Fig. 2.

The imperfect mismatch due to the mismatched GVDs is more obvious in the frequency components far away from the center frequency of the ultrashort pulse. There exists an acceptance bandwidth limited by the mismatched GVDs for which phase cannot be effectively matched. The acceptance bandwidth governed by GVD in the low-drive regime is defined as follows:

The intensity of SH pulses is given by

$$I_{SH} \propto \sin c^2(\Delta kL/2), \quad (6)$$

where L is the thickness of the crystal and Δk is the total phase mismatch. Combined with Eq. (5), the acceptance bandwidth for a crystal of thickness L is defined by

$$\Delta\omega_{JS} = \sqrt{\frac{\pi}{(2\beta_{22} - \beta_{21})L}}, \quad (7)$$

which corresponds to $I_{SH} = 0.405 I_{SHmax}$. Eq. (7) allows us to estimate the acceptance bandwidth in both phase- and group-velocity-matched SHG.

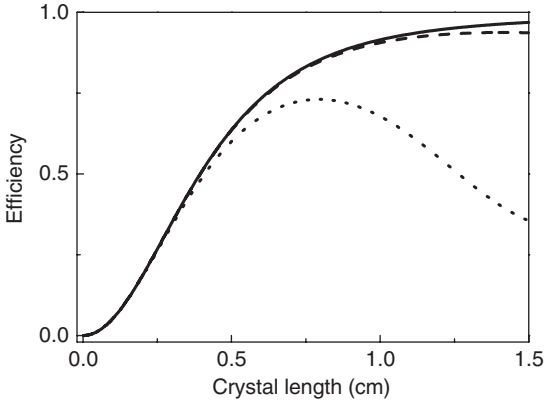

Fig. 2. Demonstration of mismatched GVD effects on conversion efficiency. For comparison, the ideal situation without GVDs of FH and SH pulses is also plotted (solid line). The dashed line represents the GVD-matched SHG ($\beta_{21} = -13\,\mathrm{fs}^2/\mathrm{mm}$, $\beta_{22} = -6.5\,\mathrm{fs}^2/\mathrm{mm}$). The dotted line represents SHG in a 12% deuterated KDP crystal ($\beta_{21} = -13\,\mathrm{fs}^2/\mathrm{mm}$, $\beta_{22} = 70\,\mathrm{fs}^2/\mathrm{mm}$). Other parameters are $T = 30$ fs, $L_{nl} = 3.5$ mm.

However, Eq. (7) does not hold true in the high-efficiency SHG, because the small-signal approximation on which Eq. (7) is based is not valid in the pump depletion regime. In order to evaluate the acceptance bandwidth of crystal in the high-efficiency SHG, we calculated the phase matching curves in the high-drive regime. The results are shown in Fig. 3. The parameter L/L_{nl} was held constant and conversion was plotted as a function of ΔkL. As the pump intensity increases, the width of the central peak narrows and the relative height of the secondary maximum increases. The narrowing of the phase matching peak will increase the importance of GVD in limiting the conversion efficiency. The tolerances of the imperfect phase mismatch thus became more restrictive at higher levels of harmonic conversion. The full width at $0.405I_{max}$ of the central peak is a function of the parameter L/L_{nl} as shown in Fig. 4. This curve provides a guide for the tolerance of imperfect phase mismatch in the high-drive regime. With this curve and Eq. (5), we can evaluate the acceptance bandwidth of crystal in the high-efficiency SHG. For example, in the case of $L_{nl} = 3.5\,\text{mm}$ ($60\,\text{GW/cm}^2$), the phase mismatch tolerance ΔkL is found to be 4.27 from Fig. 4. According to Eq. (5), the acceptance bandwidth of crystal can be determined by

$$\Delta\lambda_{JS}\sqrt{L} = 31\,\text{nm}\,\text{cm}^{1/2}. \tag{8}$$

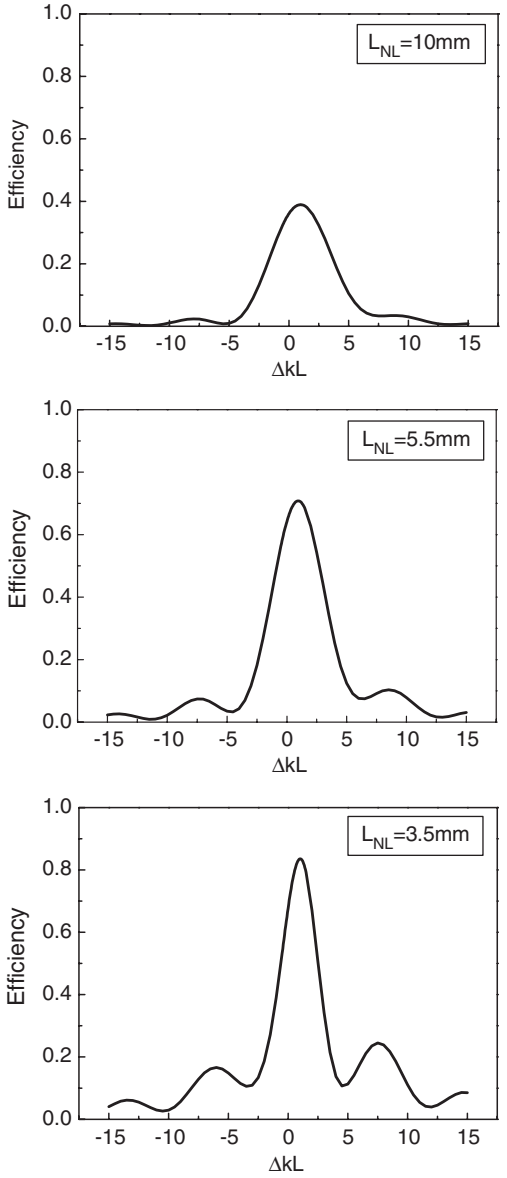

Fig. 3. Phase matching tuning curves under different pump intensity. Other parameters are $T = 30\,\text{fs}$, $L_{nl} = 3.5\,\text{mm}$, $\beta_{21} = -13\,\text{fs}^2/\text{mm}$, $\beta_{22} = -6.5\,\text{fs}^2/\text{mm}$.

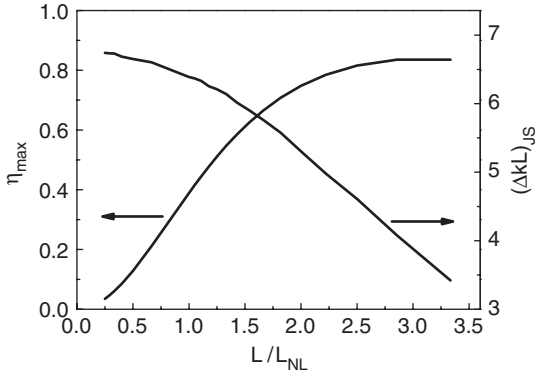

Fig. 4. Full width at $0.405I_{max}$ of the central peak of the phase matching tuning curve and peak conversion efficiency as functions of the product of reciprocal characteristic nonlinear length and crystal length.

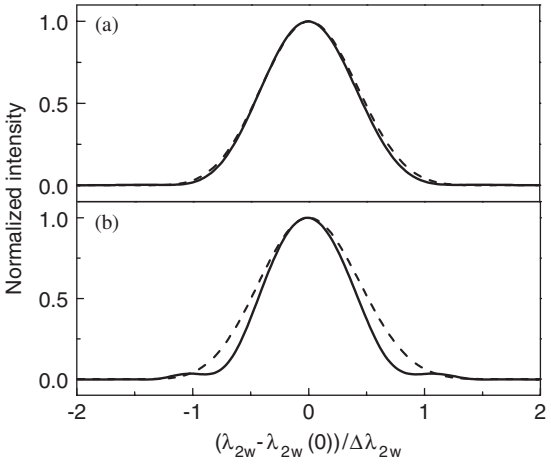

Fig. 5. Numerical results of the output SH spectra for different values of FH bandwidth: (a) $\Delta\lambda_{FH} = 31\,\text{nm}$ and (b) $\Delta\lambda_{FH} = 54\,\text{nm}$. For comparison, the ideal SH spectra under infinite acceptance bandwidth are also illustrated (dashed line). Other parameters are $L = 1\,\text{cm}$, $L_{nl} = 3.5\,\text{mm}$, $\beta_{21} = -13\,\text{fs}^2/\text{mm}$, $\beta_{22} = -6.5\,\text{fs}^2/\text{mm}$.

In order to verify our results, we calculated the output SH spectra for different input bandwidths of FH pulses, as shown in Fig. (5). For comparison, the ideal SH spectra under infinite acceptance bandwidth are also illustrated. As expected, the SH spectrum is identical to that in neglecting GVD when the FH bandwidth is relatively small (as shown in Fig. 5(a)). For a 10-mm long crystal, GVD will start to limit the output SH spectra significantly if the FH bandwidth is larger than 31 nm (as shown in Fig. 5(b)).

It is worth noting that the present acceptance bandwidth defined by Eq. (8) is under a condition of high efficiency. Compared to the conventional definition based on the small-signal approximation, this definition is much closer to the practical application of design. For efficient SHG of a femtosecond laser with bandwidth $\Delta\lambda$, the crystal length L can be directly determined by Fig. 4 and Eq. (5).

4. Conclusion

In conclusion, we have numerically studied the high-efficiency SHG of femtosecond pulses in the both PM and GVM structures. The spectral characteristics of the generated SH pulses and its conversion efficiency in the strong pump regime are investigated in detail. The acceptance bandwidth governed by GVD in the high-efficiency SHG is redefined. The conclusion is closer to the practical application of design.

References

[1] E. Sidick, A. Knoesen, A. Dienes, Ultrashort-pulse second-harmonic generation in quasi-phase-matched dispersive media, Opt. Lett. 19 (1994) 266–268.
[2] A.M. Weiner, Effect of group velocity mismatch on the measurement of ultrashort optical pulses via second harmonic generation, IEEE J. Quantum Electron. 19 (8) (1983) 1276–1283.
[3] O.E. Martinez, Achromatic phase matching for second harmonic generation of femtosecond pulses, IEEE J. Quantum Electron. 25 (12) (1989) 2464–2468.
[4] G. Szabo, Z. Bor, Broadband frequency doubler for femtosecond pulses, Appl. Phys. B 50 (1990) 51–54.
[5] B.A. Richman, S.E. Bisson, R. Trebino, E. Sidick, A. Jacobson, Efficiency broadband second-harmonic generation by dispersive achromatic nonlinear conversion using only prism, Opt. Lett. 23 (7) (1998) 497–499.
[6] P. Baum, S. Lochbrunner, E. Riedle, Tunable sub-10-fs ultraviolet pulses generated by achromatic frequency doubling, Opt. Lett. 29 (14) (2004) 1686–1688.
[7] M. Brown, Increased spectral bandwidths in nonlinear conversion process by use of multicrystal designs, Opt. Lett. 23 (20) (1998) 1591–1593.
[8] S. Ashihara, T. Shimura, K. Kuroda, Group-velocity matched second-harmonic generation in tilted quasi-phase-matched gratings, J. Opt. Soc. Am. B 20 (5) (2003) 853–856.
[9] G.Y. Wang, E.M. Garmire, High-efficiency generation of ultrashort second-harmonic pulses based on the Cerenkov geometry, Opt. Lett. 19 (4) (1994) 254–256.
[10] X. Xiao, C. Yang, S. Gao, et al., Analysis of ultrashort-pulse second0harmonic generation in both phase- and group-velocity-matched structures, IEEE. J. Quantum Electronics 41 (1) (2005) 85–93.
[11] S. Ashihara, T. Shirnura, K. Kuroda, et al., Group-velocity-matched cascaded quadratic nonlinearities of femtosecond pulses in periodically poled Mgo:$LiNbO_3$, Opt. Lett. 28 (16) (2003) 1442–1444.
[12] L.E. Nelson, S.B. Fleischer, G. Lenz, E.P. Ippen, Efficiency frequency doubling of a femtosecond fiber laser, Opt. Lett. 21 (21) (1996) 1759–1761.
[13] X. Liu, L.J. Qian, F.W. Wise, Efficient generation of 50-fs red pulses by frequency doubling in LiB_3O_5, Opt. Commun. 144 (1997) 265–268.
[14] N.E. Yu, J.H. Ro, M. Cha, S. Kurimura, T. Taira, Broadband quasi-phase-matched second-harmonic generation in MgO-doped periodically poled $LiNbO_3$ at communications band, Opt. Lett. 27 (12) (2002) 1046–1048.
[15] M.S. Webb, D. Eimerl, S.P. Velsko, Wavelength insensitive phase-matched second-harmonic generation in partially deuterated KDP, J. Opt. Soc. Am. B 9 (7) (1992) 1118–1127.
[16] H. Zhu, T. Wang, W. Zheng, P. Yuan, L. Qian, Efficient second harmonic generation of femtosecond laser at 1 μm, Opt. Exp. 12 (2004) 2150–2155.
[17] R.C. Miller, Second harmonic generation with a broadband optical maser, Phys. Lett. 26A (5) (1968) 177–178.